Multiphoton Ionization and Dissociation of Diazirine: A Theoretical and Experimental Study†

Igor Fedorov, Lucas Koziol, Andrew K. Mollner, Anna I. Krylov,* and Hanna Reisler*

Department of Chemistry, University of Southern California, Los Angeles, California 90089-0482

Received: January 8, 2009; Revised Manuscript Received: February 26, 2009

Multiphoton ionization and dissociation processes in diazirine have been studied experimentally via 304−325 nm two-photon absorption and theoretically by using the EOM-CCSD and B3LYP methods. The electronic structure calculations identified two excited valence states and four Rydberg states in the region 4.0−8.5 eV. In one-photon excitation, the strongest absorption is to the $2^1A_1(3p_x \leftarrow n)$ Rydberg state, whereas in two-photon absorption at comparable energies the first photon excites the low-lying 1^1B_2 ($\pi^* \leftarrow n$) valence state, from which the strongest absorption is to the dissociative valence 1^1A_2 ($\pi^* \leftarrow \sigma_{NN}$) state. The diazirine ion is calculated to be rather unstable, with a binding energy of only 0.73 eV and a geometry that resembles a weakly bound $CH_2^+\cdots N_2$ complex. In the experimental studies, resonance-enhanced multiphoton ionization (REMPI) experiments show no ions at the parent diazirine mass but only CH_2^+ ions from dissociative photoionization. It is proposed that weak one-photon absorption to the 1^1B_2 state is immediately followed by more efficient absorption of another photon to reach the 1^1A_2 state from which competition between ionization and fast dissociation takes place. Strong signals of CH^+ ions are also detected and assigned to 2 + 1 REMPI via the $D^2\Pi$ ($v' = 2$) ← ← $X^2\Pi$ ($v'' = 0$) two-photon transition of CH fragments. Velocity map CH^+ images show that CH(X, $v'' = 0$, N'') fragments are born with substantial translational energy, indicating that they arise from absorption of two photons in diazirine. It is argued that two-photon processes via the 1^1B_2 intermediate state are very efficient in this wavelength range, leading predominantly to dissociation of diazirine from the 1^1A_2 state. The most likely route to CH(X) formation is isomerization to isodiazirine followed by dissociation to CH + HN_2. In agreement with other theoretical papers, we recommend revisions of the heats of formation of diazirine and diazomethane.

1. Introduction

Diazirine (c-CH_2N_2) belongs to the family of isoelectronic molecules known as "16-electron molecules", which have attracted considerable attention for decades because of the inherent complexity of their photodissociation dynamics and certain similarities in their properties.[1,2] In addition, HNCO, H_2CNN, and H_2CCO, all members of this family, are known to have structural isomers.[1−16]

Of these molecules, the least studied is the H_2CN_2 group, mainly due to the instability of its prototype member, diazomethane, and its cyclic counterpart diazirine. Recently, it has become possible to produce stable molecular beams of these species, and studies of their photophysics and photochemistry in highly excited states have begun, aided by high-level electronic structure calculations. In previous papers, we described the two-photon excitation of diazomethane to 3p Rydberg states and discussed its electronic structure and couplings among its excited states.[17,18] In the present Article, we report first results on the two-photon dissociation of diazirine, specifically the formation of CH products, as well as electronic structure calculations on its excited and ionized states.

Diazirines contain a three-membered ring composed of one carbon atom and two double-bonded nitrogen atoms. Although diazomethane had been known since the 1920s, diazirines were first synthesized only in the 1960s.[19−22] However, due to their structural uniqueness and their roles as precursors of carbenes, much has been learned since then about their spectroscopy, photochemistry, and thermal decomposition.[22] For the prototype diazirine (c-CH_2N_2), the simplest member of the group, the lowest lying UV absorption bands were assigned to the structured $1^1B_2 \leftarrow 1^1A_1$ ($\pi^* \leftarrow n$) system with a band origin at 31 187 cm^{-1} (320.65 nm).[21,23] Its VUV absorption spectrum shows an intense, structureless band centered at 145−185 nm as well as diffuse structures at ∼120−143 nm.[24] The vertical (adiabatic) ionization energy (IE) of diazirine was determined experimentally at 10.75 eV (10.3 eV), and the ion's low-lying excited states are at 13.25 eV (12.8 eV) and 14.15 eV (14.15 eV).[25] Paulett and Ettinger reported the 298 K heat of formation of diazirine $\Delta H_f\,^\circ_{298} = 79.3$ kcal/mol,[26,27] whereas Laufer and Okabe obtained $60.6 < \Delta H_f\,^\circ_{298} \leq 66$ kcal/mol.[24]

Although significant experimental work has been carried out since the 1960s, the level of theoretical studies during this early period was too low to provide reliable information on excited states. With the availability of high-level electronic structure computer codes, a renewed effort to elucidate the electronic structure of diazirines/diazo compounds and their decomposition mechanisms was initiated in the 1990s.[10−13,28−30] The molecular structure of c-CH_2N_2, its related cation, and its ionization energy were the subject of several investigations.[31,32] Electronically excited states and energy differences among isomers were also calculated.[13,28]

Whereas several aspects of diazirine's photochemistry on the lowest excited state 1^1B_2 have been discussed,[10,13,33] little is known from experiment and theory about photodissociation on higher electronic states, and in particular about multiphoton

† Part of the "Robert Benny Gerber Festschrift".

* Corresponding authors. E-mail: reisler@usc.edu (H.R.); krylov@usc.edu (A.I.K.).

10.1021/jp900204g CCC: $40.75
Published on Web 04/02/2009

dissociation pathways. By combining high-level electronic structure calculations and photofragment laser spectroscopic experiments in molecular beams, we were able to investigate the photodissociation of c-CH_2N_2 following two-photon absorption. In the only previous molecular beam study, diazirine was excited to the $1^1B_2 \leftarrow 1^1A_1$ origin band, and fluorescence, tentatively assigned to emission from high vibronic levels of the excited 1^1B_2 state of the singlet methylene product, was observed.[34]

We have adapted the traditional preparation method of diazirine[20,35] to molecular beam studies and used resonance enhanced multiphoton ionization (REMPI) complemented by dc slice velocity map imaging (VMI)[36] to detect CH ($X^2\Pi$) photodissociation fragments. Specifically, CH products from two-photon dissociation were detected by 2 + 1 REMPI at the dissociation wavelength (one-color experiment) using the $D^2\Pi$ ($v' = 2$) $\leftarrow\leftarrow$ $X^2\Pi$ ($v'' = 0$) intermediate transition (where the double arrow indicates two-photon transition). The dc sliced images of CH^+ ions were anisotropic and typical of those of a perpendicular transition and fast dissociation. Several channels are discussed as possible sources of CH($X^2\Pi$) fragments, and the results suggest that the predominant pathway is two-photon absorption by the parent molecule followed by isomerization to isodiazirine and subsequent dissociation to CH + HN_2.

2. Experimental Details

The experimental arrangement has been described before,[17,18,37,38] and therefore only procedures that have changed are discussed in detail. Diazirine (c-CH_2N_2) was synthesized in the same glass vacuum line that was used in the synthesis of diazomethane.[20,39] A mixture containing ~1.5% c-CH_2N_2 in helium at a backing pressure of ~2 atm was introduced into the source chamber of the differentially pumped vacuum apparatus through a pulsed piezoelectric nozzle (10 Hz, 0.5 mm diameter). The rotational temperature of the skimmed molecular beam was estimated at ~10 K on the basis of expansion conditions and previous results. The diazirine/He sample survived for several days until depleted by use.

REMPI spectra were recorded by integrating separately ion peaks of appropriate masses as a function of laser excitation wavelength. The UV laser beam was the linearly polarized radiation from a Continuum Nd:YAG-pumped dye laser (Surelite III/ND6000) using rhodamine 610 dye (Exciton). The dye laser output was frequency-doubled (Inrad Autotracker III), producing UV pulses with maximum energy of 3.0 mJ at a repetition rate of 10 Hz. The laser radiation was focused with a 40 cm focal length (f.l.) lens at the center of the ionization region. Wavelength calibration was accomplished by using atomic carbon lines observed in 2 + 1 REMPI.[40]

Ion images of CH^+ were obtained by using the dc slice variant of VMI.[36] CH^+ ions produced by 2 + 1 REMPI via the $D^2\Pi$ ($v' = 2$) $\leftarrow\leftarrow$ $X^2\Pi$ ($v'' = 0$) transition were extracted and accelerated by the ion optics toward a 42 mm MCP detector coupled to a P47 phosphor screen (Burle Electro-optics, Inc.). Using a home-built pulser, a high voltage (~2 kV) pulse of ~5 ns fwhm was generated and applied to the MCP detector to select only the central slice of the CH^+ ion cloud. Images on the detector were recorded with a CCD camera (Imager 3, 12 bit, LaVision, 1280 × 1024 pixel array), averaged, and processed using the DaVis package (LaVision) that included event counting. CH^+ ion velocity distributions were obtained directly from the recorded sliced images as described elsewhere.[36] CH ($X^2\Pi$ ($v'' = 0$, N'')) photofragment translational energy distributions were obtained by integrating the experimental images over all angles and converting velocity to energy distributions. For energy calibration, photoelectrons obtained by NO ionization via the $A^2\Sigma^+$ state were used.[37]

Diazirine was produced in a glass reactor that was charged with 15.0 g of $3CH_2(NH_2)_2 \cdot 4H_2SO_4$, in powder form, and a NaCl/ice mixture maintained at −15 to −10 °C. $3CH_2(NH_2)_2 \cdot 4H_2SO_4$ was prepared according to the method of Ohme and Schmitz.[20,35] The reactor was submerged in an external salt/ice bath at the same temperature. A pressure-equalized addition funnel isolated from the reactor by greaseless Teflon/glass high vacuum valves was charged with 150 mL of NaOCl solution (10−14% by weight) and 30 mL of NaOH (~25 M). The reactor and the addition funnel were evacuated, and the solutions were degassed. The NaOCl/NaOH solution was then added dropwise over the course of 10 min to the reactor. The resulting c-CH_2N_2 was purified by passing the gas though two traps held at −78 °C with a dry ice/ethanol slush and was collected in a 12 L glass flask housed in a steel mesh box and protected from exposure to light. The pressure of c-CH_2N_2 was kept at less than 30 Torr. The purity of the diazirine sample was assessed from its IR and UV spectra, which were in good agreement with published spectra[21,39,41] and contained negligible amounts of impurities.

We wish to emphasize that c-CH_2N_2 is a toxic and hazardous gas, which can decompose explosively and spontaneously, and thus appropriate safety precautions must be taken. c-CH_2N_2 should be handled only at low pressures and on a small scale. At no time should the gas be allowed to condense into the liquid phase. Throughout our experiments, a pressure of 30 Torr was never exceeded. Safety equipment (safety shields, safety glasses, face shields, leather gloves, and protective clothing, such as leather suits, Kevlar sleeves, and earplugs) must be used at all times. Care must be taken to avoid known triggers of c-CH_2N_2 decomposition such as intense light and abrupt changes in temperature, pressure, and phase.

3. Computational Studies of the Electronically Excited and Ionized States of Diazirine

The equilibrium geometry and vibrational frequencies of neutral diazirine ground state were calculated by CCSD(T)[42−44] using the cc-pVTZ basis[45] and by B3LYP[46] using the 6-311G(2df,p) basis. The equilibrium geometry of the cation was calculated using B3LYP/6-311G(2df,p). Vertical excitation energies were calculated using EOM-CCSD[47−51]/6-311(3+,+)G* at the B3LYP optimized geometry. This basis set was derived from 6-311G* by adding three diffuse sp functions to heavy atoms and one diffuse s function to hydrogen. The assignment of valence and Rydberg character to the excited states was based on: (i) the symmetry of the transition, (ii) leading EOM-CCSD amplitudes and character of corresponding HF orbitals, and (iii) the second moments $\langle X^2 \rangle$, $\langle Y^2 \rangle$, and $\langle Z^2 \rangle$ of the EOM-CCSD electron density. The character of the HF orbitals was determined using the Molden interface.[52] All EOM-CCSD excited states were dominated by single excitations.

The excited valence states 1^1B_2 ($\pi^* \leftarrow$ n) and 1^1A_2 ($\pi^* \leftarrow \sigma_{NN}$) were optimized by EOM-CCSD/6-311G** under C_{2v} constraint using analytic gradients.[53] For the lowest state, 1^1B_2 ($\pi^* \leftarrow$ n), the optimized structure is a true minimum as confirmed by vibrational frequency calculations. For the 1^1A_2 ($\pi^* \leftarrow \sigma_{NN}$) state, we were not able to perform frequency calculations in this basis because of the limitations of the finite differences code and the large density of states in this energy range. To validate the structure of this state, we optimized the geometry starting from the C_1 distorted structure and computed

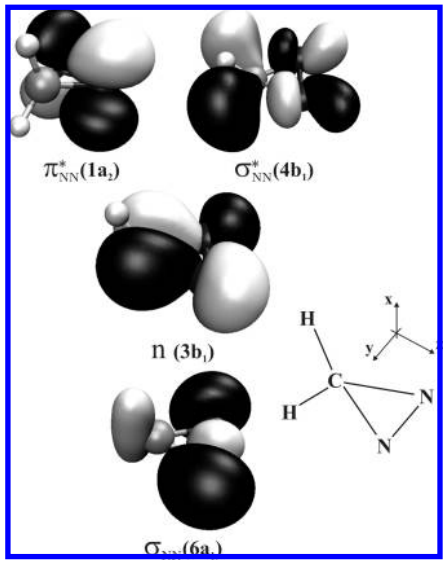

Figure 1. Molecular orbitals relevant to ground and excited electronic states of c-CH_2N_2. The three-membered ring lies in the *yz* plane, with the *z*-axis coinciding with the C_2 symmetry axis.

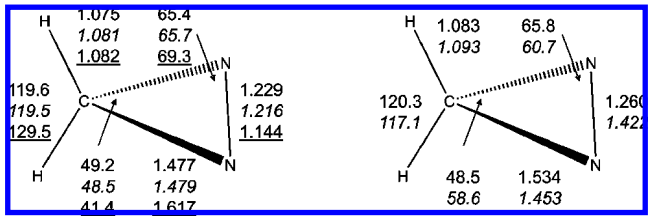

Figure 2. Left panel: Ground-state equilibrium structures (Å and deg) of diazirine for the neutral (1^1A_1) at CCSD(T)/cc-pVTZ (normal print) and B3LYP/6-311G(2df,p) (italics) and for the cation, $1^2B_1(\infty \leftarrow n)$, at B3LYP/6-311G(2df,p) (underlined). The corresponding nuclear repulsion energies are 64.158275, 64.295975, and 62.797366 hartree, respectively. Right panel: Excited-state equilibrium structures for the $1^1B_2(\pi^* \leftarrow n)$ and $1^1A_2(\pi^* \leftarrow \sigma_{NN})$ excited states at EOMCCSD/6-311G** shown in normal and italics, respectively. The corresponding nuclear repulsion energies are 62.313876 and 61.730487 hartree. Experimental parameters of the neutral ground state are: r_{C-N}, 1.482 ± 0.003 Å; r_{N-N}, 1.228 ± 0.003 Å; r_{C-H}, 1.09 ± 0.02 Å; ∠HCH, 117 ± 2°.[56]

frequencies using the smaller 6-31G* basis. This calculation produced a similar C_{2v} structure and no negative frequencies.

All optimizations, frequencies, and excited-state calculations were performed using the Q-Chem[54] and ACES II[55] electronic structure programs.

The electronic configuration of the ground state (1^1A_1) of diazirine is:

$$[\text{core} + \text{low-lying}]^{16}(6a_1)^2(2b_2)^2(3b_1)^2(1a_2)^0(4b_1)^0 = [\text{core} + \text{low-lying}]^{16}(\sigma_{NN})^2(\pi_{NN})^2(n)^2(\pi^*_{NN})^0(\sigma^*_{CN})^0$$

where "core + low-lying" refers to the 1s core orbitals and combinations of σ_{CN} and π_{NN} orbitals that are not involved in excitations. Relevant molecular orbitals are shown in Figure 1. The CNN ring lies in the *yz* plane with the *z* axis coinciding with the C_2 symmetry axis. The equilibrium geometries of diazirine in its ground neutral and cation states are shown in Figure 2, and the geometries of the excited states are given in Table 1. The neutral ground-state geometry agrees well with experimental values.[56]

The first ionization removes an electron from the highest-occupied molecular orbital (HOMO), which is the $3b_1$ orbital denoted as n in Figure 1. This orbital features σ-type bonding between an atomic p orbital on carbon and out-of-phase s orbitals on the nitrogens (see Figure 1). The geometry change upon ionization from this orbital is consistent with a weakening bonding interaction in the CN bonds; consequently, the cation resembles a weakly bound $N_2\cdots CH_2^+$ as described before.[31] Indeed, at the CCSD/6-311G(2df,p) level of theory, the cation lies only 0.73 eV (16.9 kcal/mol) below the $N_2 + CH_2^+$ asymptote. The vertical IE calculated at the B3LYP neutral geometry with the EOM-IP-CCSD/6-311G(2df,p) method is 10.71 eV. This agrees well with the experimental value;[25] triples corrections are not required for this system. The Rydberg states are expected to have structures similar to the cation and thus should be weakly bound.

The vertical excitation energies, their leading configuration state functions, and one-photon oscillator strengths are summarized in Table 2, along with oscillator strengths for transitions from the 1^1B_2 state to higher electronic states. One-photon vertical excitations from the ground state show that the strongest excitation is to the $3p_x$ Rydberg state.

Transition dipole moments were also calculated between excited states in a single EOM-CCSD calculation. This allowed us to obtain oscillator strengths specifically from the 1^1B_2 ($\pi^* \leftarrow$ n) state to the other EOM states.

The lowest excited state is a valence 1^1B_2 ($\pi^* \leftarrow$ n) excitation at 4.27 eV (293 nm). Well separated from this state, there is a cluster of states between 7.2 and 8.0 eV (174−156 nm); these are the $n = 3$ Rydberg states and the valence 1^1A_2 ($\pi^* \leftarrow \sigma_{NN}$) state. Absorption to these states agree reasonably well with the measured absorptions spectrum of diazirine at 165−145 nm.[24]

The oscillator strengths in excitation from the $^1B_2$ state show that the dominant transition is to the second valence state, 1^1A_2, rather than to the Rydberg states. The oscillator strength for the $1^1A_2 \leftarrow 1^1B_2$ transition is about an order of magnitude greater than that for $1^1B_2 \leftarrow 1^1A_1$ excitation, implying high probability for a two-photon transition via the intermediate 1^1B_2 state. Excitation to $^1A_2$ is forbidden in one-photon transition from the ground state, but is allowed in two-photon excitation via the $^1B_2$ state.

Excitation to the 1^1A_2 ($\pi^* \leftarrow \sigma_{NN}$) state removes an electron from a bonding orbital along NN (Figure 1) and places it into the π^* orbital, which is antibonding along NN. Both orbitals have electron density localized along the NN bond, and thus the excitation doubly weakens this bond.

Comparing geometries of the $^1A_2$ and ground state reveals elongation of the NN bond by 0.22 Å, which is very close to a single N−N bond length (1.45 Å), and opening of the NCN angle by approximately 9°. The CN bond length decreases only slightly, by 0.024 Å. Even though the geometry optimization produces a stable structure, the considerable reduction of the formal bonding character of this state suggests a small barrier to dissociation and nearly dissociative character. Moreover, the elongated NN bond may facilitate isomerization to isodiazirine in which the NN bond is a single bond (see below). The limitations of the employed single-reference methods do not allow us to characterize the potential energy surface (PES) too far from the Franck−Condon region.

This state was also found to be bound by the CASSCF calculations of Arenas et al.,[13] who performed surface-hopping calculations to model photoinduced dynamics on this state, referred to by them as S_2. They reported fast (~40 fs) radiationless relaxation to the 1^1B_2 state (S_1 in their notation)

TABLE 1: Calculated Equilibrium Structures for the Ground, 1^1B_2, and 1^1A_2 Valence States of the Neutral and the Ground State of the Cation

	1^1A_1[a]	1^1B_2 ($\pi^* \leftarrow$ n)[c]	1^1A_2 ($\pi^* \leftarrow \sigma_{NN}$)[b]	1^2B_1[c]
E_{nuc} (hartree)	64.158275 64.295975	62.313876	61.730487	62.797366
r_{C-N} (Å)	1.477 1.479	1.534	1.453	1.617
r_{N-N} (Å)	1.229 1.216	1.260	1.422	1.144
r_{C-H} (Å)	1.075 1.081	1.083	1.093	1.082
∠HCH (deg)	119.6 119.5	120.3	117.1	129.5
∠NNC (deg)	65.4 65.7	65.8	60.7	69.3
∠NCN (deg)	49.2 48.5	48.5	58.6	41.4

[a] Upper values calculated using CCSD(T)/cc-pVTZ, lower values using B3LYP/6-311G(2df,p), respectively. Experimental geometrical values: r_{C-N}, 1.482 ± 0.003 Å; r_{N-N}, 1.228 ± 0.003 Å; r_{C-H}, 1.09 ± 0.02 Å; ∠HCH, 117 ± 2°.[56] [b] Values calculated using EOM-CCSD/6-311G**. [c] B3LYP/6-311G(2df,p).

TABLE 2: Vertical Excitation Energies (ΔE_{vert}, eV), Oscillator Strengths (f_L)/(Oscillator Strengths from 1^1B_2 State), Dipole Strengths (μ, atomic units), and Changes in Second Dipole Moment of Charge Distributions ($\Delta\langle R^2\rangle$, squared atomic units) for the Excited States of c-CH_2N_2 at EOM-CCSD/6-311(3+,+)G*[a]

state	ΔE_{vert}	f_L	μ_{tr}^2	$\Delta\langle X^2\rangle$	$\Delta\langle Y^2\rangle$	$\Delta\langle Z^2\rangle$
$1^1B_2(\pi^* \leftarrow$ n)	4.27	0.004/(-)	0.037	0	1	−2
$1^1B_1(3s \leftarrow$ n)	7.32	0.0006/(0)	0.003	9	17	12
$1^1A_2(\pi^* \leftarrow \sigma_{NN})$	7.61	0/(0.059)	0	−1	1	−1
$2^1A_1(3p_x \leftarrow$ n)	7.86	0.099/(0.013)	0.516	25	8	7
$2^1B_1(3p_z \leftarrow$ n)	7.88	0.0210/(0)	0.021	6	11	36
$2^1A_2(3p_y \leftarrow$ n)	7.97	0/(0.015)	0	8	33	9

[a] At the B3LYP/6-311G(2df,p) optimized geometry; $E_{CCSD} = -148.417293$ hartree.

via a conical intersection followed by dissociation to methylene and N_2. However, the low level of theory employed in their work (i.e., small basis, considering only valence states, no dynamical correlation included) can adversely affect their results. For example, ref 13 reported unbound equilibrium structure for the 1^1B_2 ($\pi^* \leftarrow$ n) state, in disagreement with our calculations and the experimental Franck−Condon progressions.[21,23]

4. Experimental Results

Our first experiments were aimed at observing the REMPI spectrum of the parent diazirine by 1 + 2 REMPI via the bound $^1B_2$ state. Figure 3a presents an action spectrum recorded at $m/e = 14$ (CH_2^+) with 1.0 mJ of 305−327 nm laser radiation focused by a 40 cm f.l. lens. The spectrum consists mainly of a structureless continuum with absorption starting at ~324.0 nm (30 860 cm^{-1}). Superimposed on this continuum are broad peaks at 321.4 nm (31 114 cm^{-1}), 318.9 nm (31 358 cm^{-1}), 317.8 nm (31 466 cm^{-1}), 315.1 nm (31 736 cm^{-1}), and 307.3 nm (32 541 cm^{-1}).

In our detection system, strong ion signals induce electrical ringing for a few hundred nanoseconds after the large ion peak reaches the detector. This results in some leakage from the intense signals of $m/e = 12$ and 13 into the $m/e = 14$ region (which is 6 times less intense), and this leakage can be seen in Figure 3a. The two sharp peaks at 313.48 and 320.33 nm were assigned to the intense 2p3p $^1S_0 \leftarrow\leftarrow$ $2p^2$ $^1D_2$ and 2p3p $^1D_2 \leftarrow\leftarrow$ $2p^2$ $^1D_2$ transitions of atomic carbon ($m/e = 12$).[40] The group of sharp peaks at 311−312.5 nm belongs to the $D^2\Pi$ ($v' = 2$) $\leftarrow\leftarrow$ $X^2\Pi$ ($v'' = 0$) transition of CH detected by 2 + 1 REMPI (see below).

The CH_2^+ action spectra were seen only at fairly high laser fluences (>0.5 mJ), and they exhibited qualitatively a greater than linear dependence on fluence. However, because of the small CH_2^+ signal, no accurate fluence dependence could be measured. No signal at $m/e = 42$ from the parent diazirine ion has been detected, suggesting that the generated c-$CH_2N_2^+$ cations are unstable. Because CH_2^+ ions are observed only at

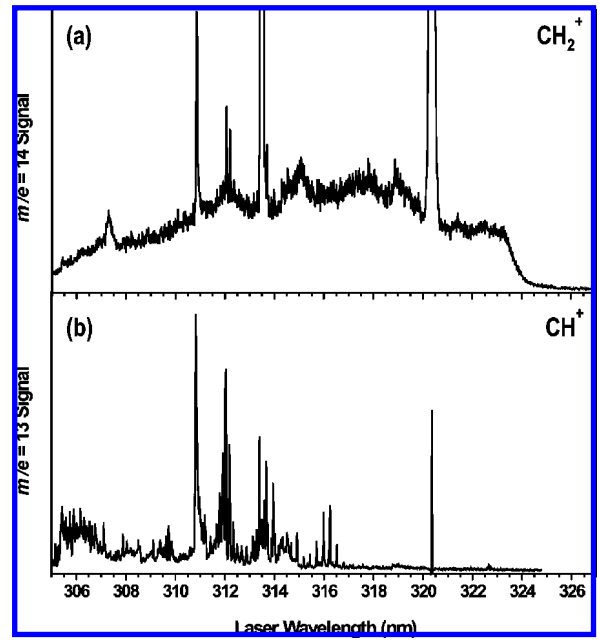

Figure 3. Survey REMPI spectra of diazirine obtained by monitoring (a) $m/e = 14$ (CH_2^+) and (b) $m/e = 13$ (CH^+) at wavelengths 305−327 nm with 0.8 and 0.3 mJ energies (40 cm f.l. lens) for (a) and (b), respectively. The spectrum in (b) is about 10 times higher in intensity than the one in (a).

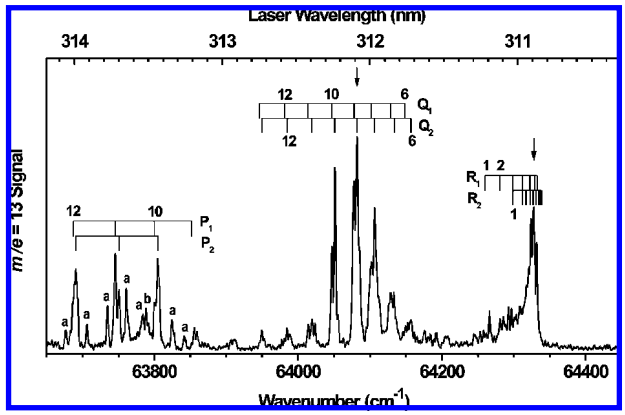

Figure 4. 2 + 1 REMPI spectrum of the CH(X) fragment (m/e = 13). Assignments of rotational CH(X, N'') levels for the $D^2\Pi$ ($v' = 2$) ←← $X^2\Pi$ ($v'' = 0$) transition are marked on top of the corresponding peaks. Lines marked "a" belong to a different band system; the line marked "b" points to the $2p3p\ ^1S_0$ ←← $2p^2\ ^1D_2$ atomic carbon transition. Arrows mark peak wavelengths at which ion images of CH^+ have been taken.

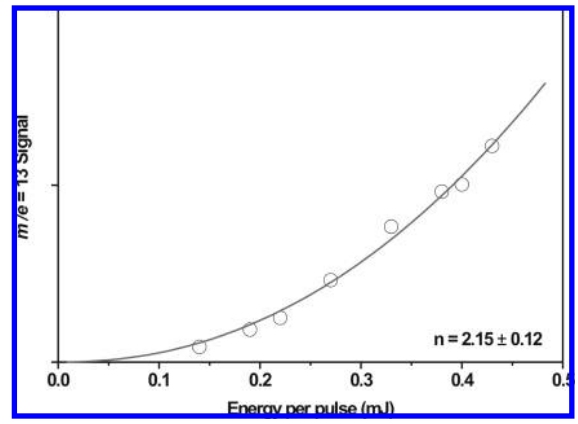

Figure 5. Fluence dependence of the CH^+ (m/e = 13) ion signal resulting from 2 + 1 REMPI through the CH $D^2\Pi$ ($v' = 2, N' \leq 9$) ← $X^2\Pi$ ($v'' = 0, N'' = 9$) transition. The dissociation wavelength was 312.10 nm, and the radiation was focused by a 40 cm f.l. lens. The signal depends on the $n = 2.15$ power of laser energy.

305−324 nm laser wavelengths, which is the region of one-photon $1^1B_2 \leftarrow 1^1A_1$ absorption, we suggest that the CH_2^+ ion fragment is formed by first excitation to 1^1B_2 followed by excitation to higher excited states leading to dissociative ionization or autoionization of a superexcited state.

Simultaneous recordings of m/e = 12 (C^+), 13 (CH^+), and 14 (CH_2^+) signals at 0.8 mJ laser fluence (40 cm f.l. lens) show that the m/e = 14 (CH_2^+) signal is about 6 times smaller than the m/e = 13 (CH^+) signal. The m/e = 12 and 13 spectral shapes are similar (see below). The c-CH_2N_2 ion mass (m/e = 42) was not observed under any conditions.

At lower laser fluences, the predominant peak is CH^+ at m/e = 13, and its action spectrum, shown in Figure 3b, is quite different from that of CH_2^+. Figure 4 shows part of the structured REMPI spectrum of CH^+ observed at 310.5−314.2 nm with 0.3 mJ laser fluence. It is noteworthy that similar spectra were observed in the multiphoton dissociation of ketene (CH_2CO),[57,58] bromoform,[59,60] and *t*-butylnitrite[58] and were assigned to the CH 2 + 1 REMPI spectrum via the CH $D^2\Pi$ ($v' = 2$) ←← $X^2\Pi$ ($v'' = 0$) transition.[58] Rotational assignments for this transition are marked in Figure 4. We use N″ for the rotational states because CH(X) reaches Hund's case (b) at low rotational levels. The dependence of the CH^+ ion signal on laser pulse energy, determined at several excitation wavelengths, is slightly higher than quadratic (Figure 5). We note that a similar but weaker REMPI spectrum was obtained by monitoring C^+ at m/e = 12; C^+ is known to be a product of predissociation of CH^+.[61,62]

Dc sliced images of CH^+ ions resulting from 2 + 1 REMPI of CH($X^2\Pi$) fragments generated in diazirine dissociation at 312.10 nm (64 082 cm^{-1}; $Q_2(N'' = 9)$) and 310.91 nm (64 328 cm^{-1}; R branch near bandhead ($N'' = 6$ and 9)) and the corresponding center-of-mass (c.m.) translational energy distributions (assuming dissociation to CH + HN_2) are displayed in Figures 6 and 7, respectively, along with their recoil anisotropy parameters β_2 and β_4. The derived translational energy distribution is broad and structureless, peaking at about 8000 cm^{-1} and extending to 20 500 ± 1000 cm^{-1}. The angular distributions were fit by the formula:

$$I(\theta) = C[1 + \beta_2 P_2(\cos\theta) + \beta_4 P_4(\cos\theta)]$$

where $P_n(x)$ is the nth Legendre polynomial, β_n is the recoil anisotropy parameter, and C is a normalization constant.[63,64]

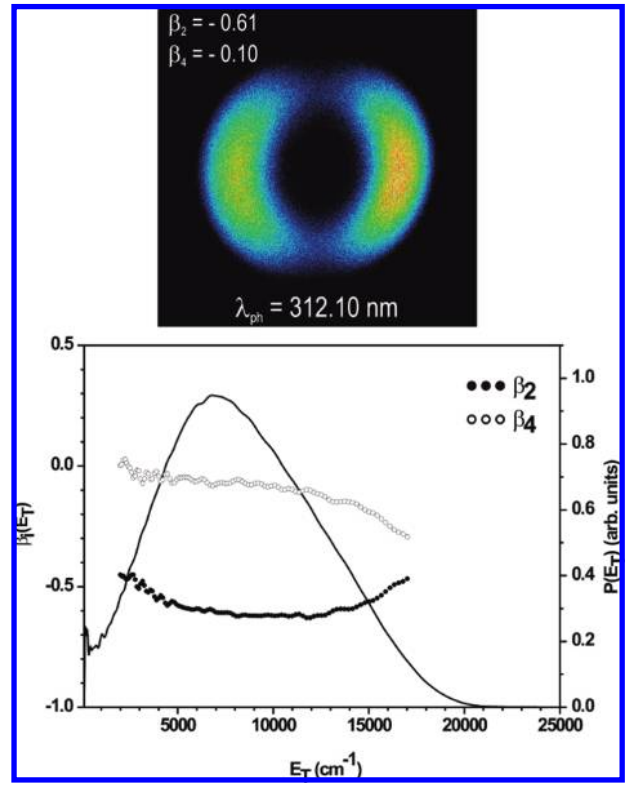

Figure 6. In the top panel is shown the image obtained in dissociation at 312.10 nm by monitoring CH(X, $v'' = 0$, $N'' = 9$). In the bottom panel, the c.m. translational energy distribution, $P(E_T)$, of the CH(X) fragments is shown (right axis), as well as the recoil anisotropy parameters $\beta_i(E_T)$ (left axis).

Both images have anisotropic angular distributions, which are well described for E_T = 5000−15 000 cm^{-1} by $\beta_2 = -0.61 \pm 0.1$ and $\beta_4 = -0.10$ at λ_{ph} = 312.10 nm, and $\beta_2 = -0.72 \pm 0.1$ and $\beta_4 \approx 0$ at λ_{ph} = 310.91 nm. The translational energy distribution does not change when the laser fluence is varied.

5. Discussion

a. Excited States and Photoionization of Diazirine. The electronic structure calculations of diazirine's excited states show that, in addition to the low-lying $1^1B_2(\pi^* \leftarrow n)$ state common to all diazirines,[21−23,28,65] there is a cluster of states in diazirine at 7.6−8.3 eV, which consists of the $n = 3$ Rydberg states (s

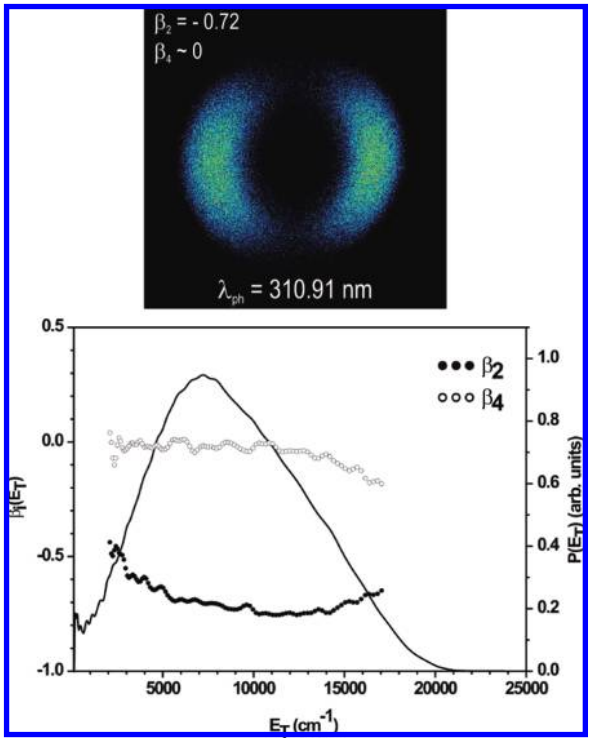

Figure 7. In the top panel is shown the image obtained in dissociation at 310.91 nm by monitoring CH(X, $v'' = 0$, $N'' = 6$ and 9), which is in the R-bandhead region. In the bottom panel, the c.m. translational energy distribution, $P(E_T)$, of the CH(X) fragments is shown (right axis), as well as the recoil anisotropy parameters $\beta_i(E_T)$ (left axis).

and p) and the 1^1A_2 ($\pi^* \leftarrow \sigma_{NN}$) valence state. The weakly bound Rydberg states appear to be pure and do not interact appreciably with nearby valence states. The most efficient one-photon absorption is expected to be to the $2^1A_1(3p_x)$ Rydberg state. The situation is quite different in two-photon excitation via the 1^1B_2 intermediate state. The oscillator strength calculations from the 1^1B_2 state suggest that the most efficient excitation is to the 1^1A_2 ($\pi^* \leftarrow \sigma_{NN}$) valence state, and this oscillator strength is greater by a factor of >4 than to the $2^1A_1(3p_x)$ and $2^1A_2(3p_y)$ Rydberg states. Thus, we believe that the main excitation process responsible for ionization and photodissociation of diazirine in our experiments is a sequential two-photon process $1^1A_2 \leftarrow 1^1B_2 \leftarrow 1^1A_1$, which accesses the bound but dissociative 1^1A_2 valence state (see section 3).

Accepting this as the main excitation process explains the high propensity for dissociative photoionization observed in the REMPI spectrum of diazirine. Both the 1^1B_2 and the 1^1A_2 states have geometries that differ significantly from the ground-state ion, and this would lead to internally excited and predissociative diazirine cations. Three photons are required for ionization of diazirine, giving rise to ions that can have >1 eV of internal energy above the 10.3 eV adiabatic ionization energy.[25] The dissociation energy of the ion is calculated at 0.73 eV above its ground state, and its geometry resembles that of the loosely bound $CH_2^+\cdots N_2$ complex (see Table 1 and Figure 2); thus, the observation that CH_2^+ fragment ions are the main photoionization products is not surprising.

b. Detection of Ionization and Dissociation Products. As discussed above, following 324−305 nm laser irradiation, multiphoton processes lead to ionization and photodissociation. The wavelength range at which CH_2^+ ions are detected coincides with the $1^1B_2 \leftarrow 1^1A_1$ structured absorption system of diazirine, but the vibronic features observed in the CH_2^+ action spectrum are much broader than those in the corresponding one-photon absorption spectrum.[21,22] This difference is rationalized by realizing that the CH_2^+ photoionization spectrum is a result of multiple photon excitation via the dissociative 1^1A_2 ($\pi^* \leftarrow \sigma_{NN}$) intermediate state. Thus, there is competition between fast dissociation and ionization, and the effective lifetime for ionization via 1 + 1 + 1 REMPI is determined by dissociation in the second intermediate state. This explains both the significant lifetime broadening and the low yield of CH_2^+ ions, which are detected only at higher laser fluences. We also note that no REMPI signal from neutral N_2 and CH_2 photofragments is detected.

The CH(X) 2 + 1 REMPI spectrum observed via the $D^2\Pi$ ($v' = 2$) ←← $X^2\Pi$ ($v'' = 0$) transition is well-known, but its analysis is complicated by severe predissociation in the upper D state.[57,59] As discussed above, similar REMPI spectra of CH(X) have been observed in multiphoton dissociation of several precursors.[57−61,66,67] In studies of photoion and photoelectron spectroscopy, it has been established that the predissociation rate in the $D^2\Pi_i$ ($v' = 2$) state increases greatly for rotational levels $N' \geq 11$ as a result of curve crossing with repulsive states,[57−59] and rotational transitions from CH(X) that terminate in $N' \geq 11$ in the D state cannot be observed. As a result of this predissociation, it is impossible to determine the effective rotational line strengths and infer populations. However, it is clear from our spectra that the decrease in the observed line intensities starts at $N'' < 11$, before fast predissociation sets in, indicating that the maximum in the rotational distribution is lower than the predissociation limit. It is also evident that the lowest rotational levels have small populations, indicating that the rotational distribution is shifted to higher rotational states and is probably nonstatistical.

Particularly striking is the similarity between the CH(X) REMPI spectra obtained in this work and the corresponding REMPI and LIF spectra of CH(X) obtained in two-photon dissociation of the isoelectronic ketene at comparable levels of parent excitation.[57−59,68] In the next section, we expand on this similarity and discuss possible dissociation mechanisms.

c. Pathways Leading to CH(X) Fragments. The most intriguing experimental finding of this work is the intense REMPI spectrum assigned to CH(X) fragments. The anisotropic angular distribution indicates that fast dissociation via a perpendicular transition is responsible for its formation. From the observation that all of the rotational branches in the CH(X) spectrum in the region 310−316 nm can be detected, we infer that the absorption by the CH(X) precursor is broad and not state specific. Although we cannot offer a definitive mechanism for the production of CH(X), we describe below several possible pathways and discuss our strong preference for one of them.

From the high CH(X) translational energies determined from the photofragment images, we conclude that this fragment must be generated by absorption of at least two photons. One-photon production of CH(X) from ground-state diazirine requires wavelengths <207 nm (48 300 cm^{-1}; 138 kcal/mol), whereas CH(X) production is observed with 314 nm excitation (31 800 cm^{-1}), and the fragments are born with substantial translational energies.

Before discussing possible reaction pathways, an assessment of the dissociation energy of diazirine to produce CH fragments is needed. The largest uncertainty derives from the value of the heat of formation of diazirine. The two experimental values (obtained over 35 years ago) differ greatly from each other, 60.6−66 kcal/mol[24] and 79.3 kcal/mol,[26,27] and each determination is associated with experimental difficulties. The NIST

TABLE 3: Calculated Values of ΔH_f° of Diazomethane and Diazirine (kcal/mol)

diazomethane		diazirine		
0 K	298 K	0 K	298 K	references
65.42, 65.68	63.18, 64.15	77.9, 74.10	76.11, 74.10	74
66.7	65.3			73
68.0	–	77.7	–	72
64.3	63.1	74.5	73.0	11,12

Chemistry Webbook[69] gives both values, and the issue has remained the subject of debate.[22,24,70−73] In the past 15 years, with theoretical methods achieving chemical accuracy, the heats of formation of diazirine and its structural isomer diazomethane (whose heat of formation is just as controversial) were calculated using high-level electronic structure methods, and a re-evaluation of the accepted values was called for.[72,73] In Table 3, we summarize the calculated heats of formation, $\Delta H_f^\circ{}_0$, which are much more convergent than the experimental ones.

Several authors have calculated heats of formation of diazomethane and diazirine through various pathways. Gordon and Kass[11,12] employed the atomization reaction and two isodesmic reactions using the G2 model chemistry, giving average values of 64.3 and 74.5 kcal/mol for $\Delta H_f^\circ{}_0$ of diazomethane and diazirine at 0 K, respectively.

Catoire[74] reported CBS-Q and G2 heats of formation for several species produced by the decomposition reactions of monomethylhydrazine. Ab initio atomization reactions and atomic heats of formation at 0 K (gas phase) were calculated, giving values of 65.4 and 65.7 kcal/mol for CBS-Q and G2 methods for diazomethane, respectively, and 78.0 and 76.0 for diazirine.

Walch[72] reported heats of formation using CASSCF methods with double-ζ Dunning basis sets for geometries, and internally contracted configuration interaction (ICCI) for energetics with double-, triple-, and quadruple-ζ Dunning bases. He recommended the value of $\Delta H_f^\circ{}_0 = 77.7$ kcal/mol for diazirine. Dixon et al.[73] reported 65.3 and 66.7 kcal/mol for the heat of formation of diazomethane at 298 and 0 K, respectively, computed using the CCSD(T) method and CBS extrapolation, which is the most accurate theoretical estimate. All calculations included zero-point corrections via harmonic frequency calculations.

For diazomethane, both G2 calculations[11,74] are within 1 kcal/mol of the result of Dixon et al.,[73] suggesting similar accuracy for the respective diazirine values. Thus, for diazomethane, the preferred theoretical value is $\Delta H_f^\circ{}_0 = 67 \pm 3$ kcal/mol, much closer to the experimental value of 67 kcal/mol recommended by Setser and Rabinovitch[75] than to values given in the NIST Chemistry Webbook.[69] Moreover, in all of the calculations, diazirine is found to lie 10 ± 1 kcal/mol above the ground state of diazomethane, allowing us to adapt the thermochemistry of diazomethane reactions to the case of diazirine (see below).[11−13,72,74] We conclude that theoretical heats of formation for diazirine are 75 ± 2 and 77 ± 2 kcal/mol at 298 and 0 K, respectively. These values are much closer to those recommended by Paulett and Ettinger,[26] than to those of Laufer and Okabe.[24]

In agreement with the calculations, in what follows we have adopted the value of 77 ± 3 kcal/mol as the heat of formation of diazirine at 0 K. We use the calculated value $\Delta H_f^\circ{}_0 = 60.8$ kcal/mol for the heat of formation of HN_2[73] and the accepted values of $\Delta H_f^\circ{}_0$ for H, CH, and $CH_2(1^1A_1)$ of 51.63,[76] 141.61 $\pm$ 0.14,[77] and 102.37 $\pm$ 0.38 kcal/mol,[77] respectively.

The most direct dissociation process leading to CH(X) formation is:

$$\text{c-}CH_2N_2(1^1A_1) + 2h\nu \rightarrow CH(X^2\Pi) + HN_2(1^2A''); \Delta H_{r0}^\circ = 125 \pm 4 \text{ kcal/mol} \quad \text{(I)}$$

The HN_2 product is metastable and is calculated to lie 9 kcal/mol above the thermochemical threshold for $H + N_2$;[78] thus the overall dissociation process is:

$$\text{c-}CH_2N_2(1^1A_1) + 2h\nu \rightarrow CH(X^2\Pi) + H(^2S) + N_2(X^1\Sigma_g^+) \quad \text{(I(a))}$$

which likely evolves in sequential steps.

To assess the feasibility of reaction I, the maximum allowed translational energy release in the CH(X) product needs to be determined. The best estimate is obtained from Figure 6, because this image was obtained for state-selected CH(X, $N'' = 9$). For this image, $2h\nu = 64\,082$ cm^{-1}, and for $N'' = 9$ of CH(X), $E_{rot} = 1300$ cm^{-1} (B(CH) = 14.457 cm^{-1}).[79] Thus, the energy required for reaction I terminating in CH(X, $N'' = 9$) is 43 900 $\pm$ 1400 cm^{-1} (125 $\pm$ 4 kcal/mol) plus 1300 cm^{-1}. Subtracting this energy from the photon energy, we obtain that the maximum allowed c.m. translational energy is $E_T = 18\,900 \pm 1400$ cm^{-1}, in good agreement with the observed value of 20 500 $\pm$ 1000 cm^{-1}.

A different route to assess the maximum allowed c.m. translational energy associated with CH(X, $N'' = 9$) in reaction I is to start with the calculated value for the dissociation of diazomethane:[80]

$$CH_2N_2(1^1A_1) \rightarrow CH_2(1^1A_1) + N_2(X^1\Sigma_g^+); \Delta H_r^\circ = 32.6 \text{ kcal/mol}$$

and then add to it the energy required to dissociate $CH_2(1^1A_1)$ to CH(X, $N'' = 9$) + H and subtract 9 kcal/mol for the formation of the HN_2 product. Taking into account the 10 kcal/mol difference between the heats of formation of diazirine and diazomethane, we obtain that reaction I should require 126 kcal/mol, which corresponds to a c.m. translational energy of $\leq$19 900 cm^{-1}, again in good agreement with the experimental result. We conclude, therefore, that our results are well explained by reaction I.

Moreover, on the basis of our results and the recent theoretical calculations, we argue that the heat of formation of diazirine at 0 K should be revised upward to 77 ± 3.0 kcal/mol and that the diazomethane value should be lower by 10 kcal/mol. We note that using the calculated value for the heat of formation of the diazirinyl radical of 117 $\pm$ 1.0 kcal/mol[74,81,82] and the calculated D_0 = 93 kcal/mol for $\text{c-}CH_2N_2(1^1A_1) \rightarrow \text{c-}CHN_2(1^2A_2) + H(^2S)$,[31] we obtain that the heat of formation of diazirine is 76 kcal/mol.

Reaction I is the only one that can generate CH(X) via absorption of two photons and thus should be the favored dissociation pathway. Inspection of the recoil anisotropy parameters shows that in the region where the intensity of CH(X) is substantial, the β_2 parameter is fairly constant and is typical of one-photon excitation via a perpendicular transition. This suggests that the anisotropy is determined largely in the second step, that is, excitation from the long-lived intermediate 1^1B_2 state to the dissociative 1^1A_2 state.

The fluence dependence of CH(X) production in these one-color experiments is not very revealing. At the fluence levels where reasonable signals are obtained (>0.15 mJ, 40 cm f.l. lens), the intensity dependence is slightly higher than quadratic; however, this dependence reflects mainly the two-photon nature

of the CH D ← X excitation rather than the 1 + 1 photon excitation process in diazirine.

The most likely mechanism of reaction I involves initial isomerization to isodiazirine, with transfer of a hydrogen atom from carbon to nitrogen:

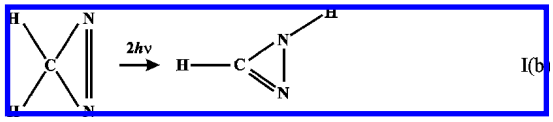

Such isomerization is in general inefficient; however, it is known that in the family of the so-called 16-electron molecules, atom shifts are unusually facile.[1,3,4,6,16,83] In particular, in the photodissociation of isotopically labeled ketene ($H_2{}^{12}C^{13}CO$), scrambling between the two carbon isotopes in the CO product has been ascribed to the formation of the cyclic intermediate oxirane, c-HCOCH,[16,83] accompanied by a hydrogen shift.

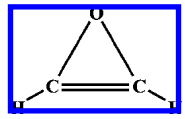

Moreover, in the two-photon excitation of ketene at comparable wavelengths (279.3 and 308 nm),[68] Ball et al. observed efficient production of CH(X) fragments and obtained their rotational distributions by LIF. The rotational distributions are bell-shaped, with widths of 10−15 *N* and maxima that shift to higher *N* values at higher excitation energies. The authors favor a mechanism in which isomerization of ketene to the formylmethylene isomer (HCCHO) via the cyclic oxirane precedes dissociation to CH(X).

In contrast, in the one-photon dissociation of ketene at 157.6 nm, the predominant product channel is CH_2 + CO, while the H + HCCO and CH + HCO channels account for less than 5% of the products.[84] One-photon dissociation, in this case, is assumed to proceed via excitation to the 3d Rydberg state, and the mechanism is different than in 1 + 1 photon excitation at about the same level of energy. It appears, therefore, that one- and two-photon dissociation processes in ketene at comparable excitation energies proceed via different mechanisms.

In conclusion, a pathway that is initiated by two-photon absorption in diazirine and evolves via isomerization and H-shift to dissociation (either simultaneously or sequentially) agrees well with our experimental observations and can also explain the high internal energies deposited in the cofragment. We point out that in the 1^1A_2 state of diazirine, the calculated N−N bond length is 1.422 Å, close to the single bond length of isodiazirine, calculated at 1.56−1.63 Å.[85−87] This should facilitate isomerization either directly on the excited state or via a conical intersection with the ground state.

Below we discuss briefly two other possible routes to CH(X) and assess their feasibility. The first is a sequential pathway initiated by breaking one C−H bond by two-photon absorption followed by one-photon dissociation of the diazirinyl radical, c-HCNN:

$$\text{c-}CH_2N_2(1^1A_1) + 2h\nu \rightarrow \text{c-HCNN}(1^2A'') + H(^2S); \quad \Delta H_r^\circ = 93 \text{ kcal/mol} \quad \text{(II(a))}$$

$$\text{c-HCNN}(1^2A'') + h\nu \rightarrow CH(X^2\Pi) + N_2(X^1\Sigma_g^+); \quad \Delta H_r^\circ = 26 \text{ kcal/mol} \quad \text{(II(b))}$$

Assuming that the maximum CH(X) translational energy allowed by the thermochemistry in each step is achieved, translational energies higher than 21 000 cm^{-1} may be observed. In step IIa, both the cyclic and the open-chain HCNN may be generated.

To date, there is no experimental information on the diazirinyl radical, but calculations show that it is a stable species, close in its heat of formation to the open-chain HCNN, HNCN, and CNNH structural isomers.[81,82,88−91] The HCNN system has recently attracted attention because of its relevance to the CH + N_2 reaction mechanism, and the facile isomerization among different structural isomers has been discussed.[81,82,88−91] Experimentally, while no studies of diazirinyl photodissociation are available, Neumark and co-workers have studied the photodissociation of jet-cooled open-chain HCNN radicals via a parallel transition at wavelengths that coincide with the photon energies used in the current experiments.[92] HCNN exhibits broad absorption features at 26 000−40 000 cm^{-1}, with an onset of dissociation at about 25 400 cm^{-1}, resulting in a broad translational energy distribution in the CH(X) radical. While this mechanism can explain the observed high translational energies, it does not explain the observed anisotropy parameter. Also, the requirement for three-photon absorption plus two photon for detection makes this pathway less likely than mechanism I, and the importance of reaction IIa needs to be established independently.

Another reaction sequence that may, in principle, lead to formation of CH(X) with high translational energies is initial one-photon dissociation on the 1^1B_2 state of diazirine to generate CH_2 fragments in one of the three lowest singlet states, followed by two-photon absorption in CH_2 to generate CH(X). We feel that such a sequence is unlikely, because (i) the one-photon $^1B_2 \leftarrow {}^1A_1$ absorption in diazirine is highly structured, and (ii) the subsequent photon absorption by the small radical CH_2 should also be structured and not necessarily coincide with the CH D ← X absorption at all wavelengths. Thus, the broad and even nature of the absorption spectrum in our studies leads us to believe that the first step involves 1 + 1 excitation to the $^1A_2$ state followed by dissociation to CH(X).

6. Summary

Multiphoton ionization and dissociation processes in diazirine have been studied both experimentally (via 304−325 nm two-photon absorption) and theoretically by using the EOM-CCSD and B3LYP methods. The electronic structure calculations identified two valence states and four Rydberg states in the region 4.0−8.5 eV. In one-photon excitation, the calculated strongest absorption is to the $2^1A_1(3p_x)$ Rydberg state, whereas in two-photon absorption at comparable energies—via the low-lying 1^1B_2 valence state, the strongest absorption is predicted to reach the dissociative valence 1^1A_2 state. The diazirine ion should be rather unstable, with a binding energy of only 0.73 eV and a geometry that resembles a weakly bound $CH_2{}^+\cdots N_2$ complex.

On the basis of the electronic structure calculations, we conclude that two-photon absorption in diazirine is very efficient. Weak absorption to the 1^1B_2 state is immediately followed by more efficient absorption of another photon to reach the 1^1A_2 state from which competition between ionization and fast dissociation takes place. Absorption of a third photon leads to

dissociative photoionization with the formation of CH_2^+ fragment ions. No parent diazirine ions are detected.

Two-photon dissociation on the 1^1A_2 state leads to efficient detection of CH(X) fragments. We propose that the most likely route to CH(X) formation is isomerization to isodiazirine followed by dissociation. This mechanism agrees well with the measured maximum in the c.m. translational energy and is similar to the proposed mechanism for formation of CH(X) in two-photon dissociation of the isoelectronic ketene.[68] Comparison between one- and two-photon dissociation at 150−170 nm would be enlightening.

In closing, and in agreement with previous theoretical papers,[11,72−75] we call for a revision of the heats of formation of diazirine and diazomethane to 77 ± 3 and 67 ± 3 kcal/mol, respectively.

Acknowledgment. We thank Karl O. Christe and C. J. Bigler Jones for their generous help in the modification of the c-CH_2N_2 synthesis procedure for molecular beam conditions, Mikhail Ryazanov for use of the ns HV pulser and help in image analysis, and Lee Ch'ng for analyzing the CH(X) REMPI spectra. This work was carried out under the auspices of the Center for Computational Studies of Electronic Structure and Spectroscopy of Open-Shell and Electronically Excited Species supported by the National Science Foundation through the CRIF: CRF CHE-0625419 + 0624602 + 0625237. Support of this work by the Chemical Sciences, Geosciences, and Biosciences Division, Office of Basic Energy Sciences, U.S. Department of Energy (to A.I.K. and H.R.) and the Air Force Office of Scientific Research (to H.R.) is gratefully acknowledged.

References and Notes

(1) Rabalais, J. W.; Mcdonald, J. M.; Scherr, V.; McGlynn, S. P. *Chem. Rev.* **1971**, *71*, 73.
(2) Jackson, W. M.; Okabe, H. *Adv. Photochem.* **1986**, *13*, 1.
(3) Mclean, A. D.; Loew, G. H.; Berkowitz, D. S. *J. Mol. Spectrosc.* **1977**, *64*, 184.
(4) Pinnavaia, N.; Bramley, M. J.; Su, M. D.; Green, W. H.; Handy, N. C. *Mol. Phys.* **1993**, *78*, 319.
(5) Moore, C. B. *Faraday Discuss.* **1995**, *102*, 1.
(6) Shapley, W. A.; Bacskay, G. B. *J. Phys. Chem. A* **1999**, *103*, 6624.
(7) Schuurman, M. S.; Muir, S. R.; Allen, W. D.; Schaefer, H. F. *J. Chem. Phys.* **2004**, *120*, 11586.
(8) Mladenovic, M.; Lewerenz, M. *Chem. Phys.* **2008**, *343*, 129.
(9) Goldberg, N.; Fiedler, A.; Schwarz, H. *Helv. Chim. Acta* **1994**, *77*, 2354.
(10) Yamamoto, N.; Bernardi, F.; Bottoni, A.; Olivucci, M.; Robb, M. A.; Wilsey, S. *J. Am. Chem. Soc.* **1994**, *116*, 2064.
(11) Gordon, M. S.; Kass, S. R. *J. Phys. Chem.* **1995**, *99*, 6548.
(12) Gordon, M. S.; Kass, S. R. *J. Phys. Chem. A* **1997**, *101*, 7922.
(13) Arenas, J. F.; Lopez-Tocon, I.; Otero, J. C.; Soto, J. *J. Am. Chem. Soc.* **2002**, *124*, 1728.
(14) Lovejoy, E. R.; Kim, S. K.; Alvarez, R. A.; Moore, C. B. *J. Chem. Phys.* **1991**, *95*, 4081.
(15) Lovejoy, E. R.; Moore, C. B. *J. Chem. Phys.* **1993**, *98*, 7846.
(16) Gezelter, J. D.; Miller, W. H. *J. Chem. Phys.* **1995**, *103*, 7868.
(17) Fedorov, I.; Koziol, L.; Li, G. S.; Parr, J. A.; Krylov, A. I.; Reisler, H. *J. Phys. Chem. A* **2007**, *111*, 4557.
(18) Fedorov, I.; Koziol, L.; Li, G. S.; Reisler, H.; Krylov, A. I. *J. Phys. Chem. A* **2007**, *111*, 13347.
(19) Paulsen, S. R. *Angew. Chem., Int. Ed.* **1960**, *72*, 781.
(20) Schmitz, E.; Ohme, R. *Chem. Ber. Recl.* **1961**, *94*, 2166.
(21) Graham, W. H. *J. Am. Chem. Soc.* **1962**, *84*, 1063.
(22) Liu, M. T. H., Ed. *Chemistry of Diazirines*; CRC Press: Boca Raton, FL, 1987.
(23) Robertson, L. C.; Merritt, J. A. *J. Mol. Spectrosc.* **1966**, *19*, 372.
(24) Laufer, A. H.; Okabe, H. *J. Phys. Chem.* **1972**, *76*, 3504.
(25) Robin, M. B.; Wiberg, K. B.; Ellison, G. B.; Brundle, C. R.; Kuebler, N. A. *J. Chem. Phys.* **1972**, *57*, 1758.
(26) Paulett, G. S.; Ettinger, R. *J. Chem. Phys.* **1963**, *39*, 825.
(27) Paulett, G. S.; Ettinger, R. *J. Chem. Phys.* **1963**, *39*, 3534.
(28) Han, M. S.; Cho, H.-G.; Cheong, B.-S. *Bull. Korean Chem. Soc.* **1999**, *20*, 1281.
(29) Ball, D. W. *THEOCHEM* **2005**, *722*, 213.
(30) Boldyrev, A. I.; Schleyer, P. V.; Higgins, D.; Thomson, C.; Kramarenko, S. S. *J. Comput. Chem.* **1992**, *13*, 1066.
(31) Puzzarini, C.; Gambi, A. *Chem. Phys.* **2004**, *306*, 131.
(32) Puzzarini, C.; Gambi, A.; Cazzoli, G. *J. Mol. Struct.* **2004**, *695*, 203.
(33) Kim, T. S.; Kim, S. K.; Choi, Y. S.; Kwak, I. *J. Chem. Phys.* **1997**, *107*, 8719.
(34) Lim, S. M.; Kim, T. S.; Lim, G. I.; Kim, S. K.; Choi, Y. S. *Chem. Phys. Lett.* **1998**, *288*, 828.
(35) Vogt, J.; Winnewisser, M.; Christiansen, J. J. *J. Mol. Spectrosc.* **1984**, *103*, 95.
(36) Townsend, D.; Minitti, M. P.; Suits, A. G. *Rev. Sci. Instrum.* **2003**, *74*, 2530.
(37) Dribinski, V.; Potter, A. B.; Fedorov, I.; Reisler, H. *Chem. Phys. Lett.* **2004**, *385*, 233.
(38) Sanov, A.; Droz-Georget, T.; Zyrianov, M.; Reisler, H. *J. Chem. Phys.* **1997**, *106*, 7013.
(39) Gambi, A.; Winnewisser, M.; Christiansen, J. J. *J. Mol. Spectrosc.* **1983**, *98*, 413.
(40) Moore, C. E. *Atomic Energy Levels*; Official Standards Reference Data Series, National Bureau of Standards 35; U.S. Goverment: Washington, DC, 1971; Vol. 1.
(41) Ettinger, R. *J. Chem. Phys.* **1964**, *40*, 1693.
(42) Purvis, G. D.; Bartlett, R. J. *J. Chem. Phys.* **1982**, *76*, 1910.
(43) Raghavachari, K.; Trucks, G. W.; Pople, J. A.; Headgordon, M. *Chem. Phys. Lett.* **1989**, *157*, 479.
(44) Watts, J. D.; Gauss, J.; Bartlett, R. J. *J. Chem. Phys.* **1993**, *98*, 8718.
(45) Dunning, T. H. *J. Chem. Phys.* **1989**, *90*, 1007.
(46) Becke, A. D. *J. Chem. Phys.* **1993**, *98*, 5648.
(47) Sekino, H.; Bartlett, R. J. *Int. J. Quantum Chem. Symp.* **1984**, *18*, 255.
(48) Koch, H.; Jensen, H. J. A.; Jorgensen, P.; Helgaker, T. *J. Chem. Phys.* **1990**, *93*, 3345.
(49) Stanton, J. F.; Bartlett, R. J. *J. Chem. Phys.* **1993**, *98*, 7029.
(50) Levchenko, S. V.; Krylov, A. I. *J. Chem. Phys.* **2004**, *120*, 175.
(51) Krylov, A. I. *Annu. Rev. Phys. Chem.* **2008**, *59*, 433.
(52) Schaftenaar, G.; Noordik, J. H. *J. Comput.-Aided Mater. Des.* **2000**, *14*, 123.
(53) Levchenko, S. V.; Wang, T.; Krylov, A. I. *J. Chem. Phys.* **2005**, *122*, 224106.
(54) Shao, Y.; Molnar, L. F.; Jung, Y.; Kussmann, J.; Ochsenfeld, C.; Brown, S. T.; Gilbert, A. T. B.; Slipchenko, L. V.; Levchenko, S. V.; O'Neill, D. P.; DiStasio, R. A.; Lochan, R. C.; Wang, T.; Beran, G. J. O.; Besley, N. A.; Herbert, J. M.; Lin, C. Y.; Van Voorhis, T.; Chien, S. H.; Sodt, A.; Steele, R. P.; Rassolov, V. A.; Maslen, P. E.; Korambath, P. P.; Adamson, R. D.; Austin, B.; Baker, J.; Byrd, E. F. C.; Dachsel, H.; Doerksen, R. J.; Dreuw, A.; Dunietz, B. D.; Dutoi, A. D.; Furlani, T. R.; Gwaltney, S. R.; Heyden, A.; Hirata, S.; Hsu, C. P.; Kedziora, G.; Khalliulin, R. Z.; Klunzinger, P.; Lee, A. M.; Lee, M. S.; Liang, W.; Lotan, I.; Nair, N.; Peters, B.; Proynov, E. I.; Pieniazek, P. A.; Rhee, Y. M.; Ritchie, J.; Rosta, E.; Sherrill, C. D.; Simmonett, A. C.; Subotnik, J. E.; Woodcock, H. L.; Zhang, W.; Bell, A. T.; Chakraborty, A. K.; Chipman, D. M.; Keil, F. J.; Warshel, A.; Hehre, W. J.; Schaefer, H. F.; Kong, J.; Krylov, A. I.; Gill, P. M. W.; Head-Gordon, M. *Phys. Chem. Chem. Phys.* **2006**, *8*, 3172.
(55) Stanton, J. F.; Gauss, J.; Watts, J. D.; Lauderdale, W. J.; Bartlett, R. J. ACES II; 1993. The package also contains modified versions of the MOLECULE Gaussian integral program of J. Almlöf and P. R. Taylor, the ABACUS integral derivative program written by T. U. Helgaker, H. J. Aa. Jensen, P. Jørgensen, and T. P. Taylor, and the PROPS property evaluation integral code of P. R. Taylor.
(56) Pierce, L.; Dobyns, V. *J. Am. Chem. Soc.* **1962**, *84*, 2651.
(57) Chen, P.; Pallix, J. B.; Chupka, W. A.; Colson, S. D. *J. Chem. Phys.* **1987**, *86*, 516.
(58) Chen, P.; Chupka, W. A.; Colson, S. D. *Chem. Phys. Lett.* **1985**, *121*, 405.
(59) Wang, Y. M.; Li, L. P.; Chupka, W. A. *Chem. Phys. Lett.* **1992**, *192*, 348.
(60) Hudgens, J. W.; Dulcey, C. S.; Long, G. R.; Bogan, D. J. *J. Chem. Phys.* **1987**, *87*, 4546.
(61) Wang, Y. M.; Li, L. P.; Chupka, W. A. *Chem. Phys. Lett.* **1991**, *185*, 478.
(62) Hechtfischer, U.; Williams, C. J.; Lange, M.; Linkemann, J.; Schwalm, D.; Wester, R.; Wolf, A.; Zajfman, D. *J. Chem. Phys.* **2002**, *117*, 8754.
(63) Zare, R. N. *Mol. Photochem.* **1972**, *4*, 1.
(64) Zare, R. N., Ed. *Angular Momentum: Understanding Spatial Aspects in Chemistry and Physics*; Wiley: New York, 1988; p 349.
(65) Robertson, L. C.; Merritt, J. A. *J. Mol. Spectrosc.* **1967**, *24*, 44.
(66) Pallix, J. B.; Chen, P.; Chupka, W. A.; Colson, S. D. *J. Chem. Phys.* **1986**, *84*, 5208.
(67) Tjossem, P. J. H.; Smyth, K. C. *Chem. Phys. Lett.* **1988**, *144*, 51.

(68) Ball, S. M.; Hancock, G.; Heal, M. R. *J. Chem. Soc., Faraday Trans.* **1994**, *90*, 523.
(69) Afeefy, H. Y.; Liebman, J. F.; Stein, S. E. Neutral Thermochemical Data. In *NIST Chemistry WebBook, NIST Standard Reference Database Number 69*; Linstrom, P. J., Mallard, W. G., Eds.; NIST: Gaithersburg, MD, 2003; http://webbook.nist.gov/.
(70) Bell, J. A. *J. Chem. Phys.* **1964**, *41*, 2556.
(71) Paulett, G. S.; Ettinger, R. *J. Chem. Phys.* **1964**, *41*, 2557.
(72) Walch, S. P. *J. Chem. Phys.* **1995**, *103*, 4930.
(73) Dixon, D. A.; de Jong, W. A.; Peterson, K. A.; McMahon, T. B. *J. Phys. Chem. A* **2005**, *109*, 4073.
(74) Catoire, L.; Swihart, M. T. *J. Propul. Power* **2002**, *18*, 1242.
(75) Setser, D. W.; Rabinovitch, B. S. *Can. J. Chem.* **1962**, *40*, 1425.
(76) Lias, S. G.; Bartmess, J. E.; Liebman, J. F.; Holmes, J. L.; Levin, R. D.; Mallard, W. G. *J. Phys. Chem. Ref. Data* **1988**, *17*, 1.
(77) Ruscic, B.; Boggs, J. E.; Burcat, A.; Csaszar, A. G.; Demaison, J.; Janoschek, R.; Martin, J. M. L.; Morton, M. L.; Rossi, M. J.; Stanton, J. F.; Szalay, P. G.; Westmoreland, P. R.; Zabel, F.; Berces, T. *J. Phys. Chem. Ref. Data* **2005**, *34*, 573.
(78) Koizumi, H.; Schatz, G. C.; Walch, S. P. *J. Chem. Phys.* **1991**, *95*, 4130.
(79) Huber, K. P.; Herzberg, G. *Molecular Spectra and Molecular Structure. Constants of Diatomic Molecules*; Van Nostrand Reinhold Co.: New York, 1979; Vol. IV.
(80) Papakondylis, A.; Mavridis, A. *J. Phys. Chem. A* **1999**, *103*, 1255.
(81) Berman, M. R.; Tsuchiya, T.; Gregusova, A.; Perera, S. A.; Bartlett, R. J. *J. Phys. Chem. A* **2007**, *111*, 6894.
(82) Harding, L. B.; Klippenstein, S. J.; Miller, J. A. *J. Phys. Chem. A* **2008**, *112*, 522.
(83) Bouma, W. J.; Nobes, R. H.; Radom, L.; Woodward, C. E. *J. Org. Chem.* **1982**, *47*, 1869.
(84) Lu, I. C.; Lee, S. H.; Lee, Y. T.; Yang, X. M. *J. Chem. Phys.* **2006**, *124*, 024342.
(85) Moffat, J. B. *J. Mol. Struct.* **1979**, *52*, 275.
(86) Alcami, M.; Depaz, J. L. G.; Yanez, M. *J. Comput. Chem.* **1989**, *10*, 468.
(87) Guimon, C.; Khayar, S.; Gracian, F.; Begtrup, M.; Pfister-Guillouzo, G. *Chem. Phys.* **1989**, *138*, 157.
(88) Manaa, M. R.; Yarkony, D. R. *J. Chem. Phys.* **1991**, *95*, 1808.
(89) Manaa, M. R.; Yarkony, D. R. *Chem. Phys. Lett.* **1992**, *188*, 352.
(90) Moskaleva, L. V.; Lin, M. C. *Proc. Combust. Inst.* **2000**, *28*, 2393.
(91) Moskaleva, L. V.; Xia, W. S.; Lin, M. C. *Chem. Phys. Lett.* **2000**, *331*, 269.
(92) Faulhaber, A. E.; Gascooke, J. R.; Hoops, A. A.; Neumark, D. M. *J. Chem. Phys.* **2006**, 124.

JP900204G